Chapter II

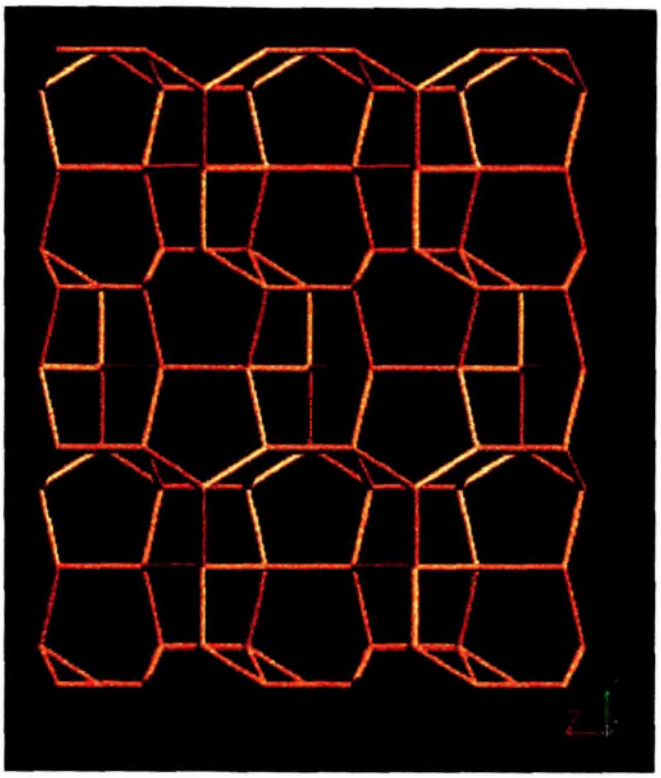

Synthesis of Ferrierite

2.1 Introduction:

Natural ferrierite was first named by *W.F. Ferrier* (Nat. Zeo. 1985, Structure code FER[1]) and is a rare and most siliceous naturally occurring zeolite. Vaughan[2] solved the crystallographic structure of mineral Ferrierite which occurs near Kamloops Lake, at British Columbia, in 1966. The structure IUPAC code FER[1] was based on five membered rings. Four such five-membered rings are linked to give [5^4] polyhedral units from which 3-D frame can be constructed. There are two types of perpendicularly intersecting channels. The main channel delineated by 10 membered ring runs along the orthorhombic *c* axis whereas the other channel which runs parallel to the *b* axis is outlined by 8 membered rings. The high bond density layers parallel to the *bc* planes are interconnected by T— O— T bonds. The resulting interlayer bond density being much lower leads to the plate-like morphology of the ferrierite crystals.

The other synthetic zeolites classified under ferrierite class are FU-9 [*Imperial Chemical Industries EP 58,529 (1982)*], ISI-6 [*US4, 578,259; Research Association for Petroleum Alternative Development, (1986)],* ZSM-35 *[Mobil Oil Corporation, US4,016,245, (1977)] and* NU-23 *[Imperial Chemical Industries, EP 103,981 (1984)].* ZSM-35 zeolite can be distinguished from natural ferrierite, on the basis of their XRD lines. A significant line at 1.133 nm (11.33 Å) present in natural ferrierite is very weak in intensity if present in these (ZSM-35) materials[3,4,5]. This has been attributed by Kokotailo *et al.*[6] to difference in cation content. FU-9 also belongs to FER-type structure[7] and the XRD pattern is similar to that reported by Vaughan[2]. It is apparent that ZSM-21 and FU-9 are unique members of FER family and possibly differ in the degree of faulting.

According to Sheddon and Whittam[7], ZSM-35 is a FER structure with fault lines perpendicular to the b axis, whereas FU-9 is closer to the theoretical structure. Table 2.1 summarizes the differences between the members of FER family

Table 2.1 Proposed differences between different members of the FER family[7]

Technique	Ferrierite (natural)	ZSM-35	FU-9
XRD lines	FER phase	FER phase	FER phase
d at 11.33 Å	strong	absent or very weak	weak
crystal morphology	irregular	thin rods	small regular crystals
Electron diffraction	faults ⊥ b	faults ⊥ b	no faults

Barrer and Marshall[8] demonstrated the first synthesis of ferrierite under hydrothermal conditions in 1964. This procedure involved the use of strontium as the inorganic cation; the synthesis temperature was 613 K and the product crystallized after 10 days. Since then a number of reports[9-11] on synthesis of ferrierite appeared. Most of them required high crystallization temperatures and FER could be obtained with low SiO_2/Al_2O_3 ratios. Winquist[12] synthesized ferrierite from gels containing Na_3PO_4 and KF, with SiO_2/Al_2O_3 ratio of 11 in the temperature range 448 - 483 K, which are significantly lower than those reported previously.

More than a decade ago Kibby *et al.*[13] reported synthesis of ferrierite using quaternary ammonium cations namely tetramethylammonium hydroxide. Since then a number of N- containing molecules and also oxygenated hydrocarbons have been used in FER synthesis (Table 2.2).

Table 2.2: Synthesis of FER structure types in presence of organics.

No.	Notation	Organic	Reference
1.	TMA-Ferrierite	Tetra Methyl Ammonium Hydroxide	13
2.	Ferrierite	2,4-Pentadione	14
3.	Ferrierite	1,4-Diaminobutane	15
4.	Ferrierite	N-methyl pyridinium	16
5.	Ferrierite	Piperidine	17
6.	Ferrierite	Glycerol	18
7.	Ferrierite	1,6-Diaminohexane	19
8.	FER type	1,3-Diaminopropane	20
9.	FER type	1,4-Diaminobutane	20
10	ZSM-35	pyrrolidine	3
11.	FER type	hexamethylene diamine	3
12.	FER type	trimethyl cetyl ammonium hydroxide	21
13.	FER type	ethylene diamine	22
14.	FER type	trimethylamine hydrochloride	23
15.	FER type	cyclohexyl amine	24
16.	FER type	4 amino-2,2,6,6-tetramethyl piperidine	25
17.	Ferrierite	1,4-Dimethyl piperidine	26
18.	FER-type	diethanolamine	27
19.	FER-type	1,4-Diaminocyclohexane	28

Gies and Gunawardane[29] first synthesized the siliceous form of ferrierite from aqueous medium. On the contrary a non aqueous route in presence of fluoride ions has been reported by Kuperman *et al.*[30] Kim *et al.*[31] succeeded in synthesizing FER in absence of inorganic cations using pyrrolidine, 1,4-diaminobutane and ethylene diamine as structure directing agents.

Number of studies reflects variety of isomorphous substitution in FER framework. Ga^{3+} has been successfully incorporated in the ferrierite structure[32,33] and recently Borade and Clearfield[34] described the synthesis of iron ferrierite, while TS-Fer titanosilicate system has been reported by Ahedi and Kotasthane[34b]

This chapter describes:

- Systematic synthesis of ferrierite using pyrrolidine and tetramethyl ammonium hydroxide as templates.
- Synthesis of ferrierite in presence of promoting media and their crystallization kinetics.

- Synthesis of ferrierite in presence of an anionic surfactant sodium bis-(2 ethylhexyl) sulphosuccinate, AOT.
- Synthesis of ferrierite in inorganic media (without template).
- Isomorphous substitution of Fe^{3+} for Al^{3+} under hydrothermal conditions.
- Isomorphous substitution of Ti^{4+} for Si^{4+} under organothermal conditions.

2.2 Experimental:

2.2.1. Synthesis of Al-FER ferrierite:

2.2.1.1. Pyrrolidine template:

The reagents used for the synthesis of aluminum analog of ferrierite are listed in Table 2.3. In typical synthesis 52.5 g sodium silicate in 25 ml distilled water was stirred with 10-ml pyrrolidine. To this solution a mixture containing 2.4 g of aluminum sulphate hexadecahydrate in 25 ml distilled water and 1.8 g of sulphuric acid in 10 ml distilled water was added. Finally the remaining quantity i.e. 30 ml of distilled water was added. The gel was stirred for ~ 2h. This gel (pH 11.5 ± 0.2) was then transferred into a 300 ml stainless steel Parr autoclave (4842, 300 ml) and heated at 433 K for 60 h. The initial gel composition was:

$$20\ Na_2O : Al_2O_3 : 37\ pyrrolidine : 66\ SiO_2 : 1460\ H_2O.$$

The autoclave was quenched, filtered, washed and product was dried at 373 K for 6-8 h. The samples with SiO_2/Al_2O_3 ratios in the range 25 - 60 were synthesized using the above method. The asynthesized form was converted to sodium form by calcining at 823 K in airflow for 18 - 20 h. the yield of the product was 9g.

2.2.1.2. Tetra methyl ammonium hydroxide system:

The reagents used for this synthesis are listed in Table 2.3. In a typical preparation a mixture of 5.3 g of sodium aluminate and 10.5 g of tetramethyl ammonium hydroxide in 50 ml distilled water was added to 71.7 g silica sol in 25 ml distilled water. The thick gel obtained was stirred until homogenous. The gel (pH 12 ± 0.2) was transferred to

stainless steel Parr autoclave (4842, 300 ml) and heated at 473 K for 24 h. The white solid crystalline mass obtained was filtered, washed and dried at 373 K, after quenching the autoclave with cold water. The occluded organic template was decomposed by subjecting the asynthesized sample to calcination in a stepwise mode at 823 K. The initial gel composition was:

$$7.8\ Na_2O : Al_2O_3 : 0.64\ (TMA)_2O : 15.26\ SiO_2 : 184\ H_2O$$

The yield was 12g.

Table 2.3: Reagents used in synthesis of Al-FER.

Reactants	Suppliers	Analysis
Pyrrolidine	SRL	99%
Tetramethyl ammonium hydroxide	SRL	25% aqueous
Silica sol	-	28% SiO_2; 2.0 % Na_2O
Sodium silicate	-	28% SiO_2; 9.0% Na_2O
Sodium aluminate	-	43.68% Al_2O_3; 39% Na_2O
Aluminum sulphate hexadecahydrate $[Al_2(SO_4)_3.16\ H_2O]$	Loba Chemie	99%
Sulphuric acid	BDH	98%
Perchloric acid	J.T. Baker	60 - 62 %
orthophosphoric acid	S.D. fine chem. ltd.	85%
Trisodium phosphate	E. Merck	99%
Fumed silica	Cab-O-Sil (Fluka AG)	99%
Potassium fluoride	Loba Chemie	99%
AOT		

2.2.1.3. Synthesis of ferrierite in promoting media:

The synthesis procedure described in section 2.2.1.1, was followed. Equimolar quantities of perchloric acid or orthophosphoric acid were added instead of sulphuric acid.

2.2.1.4. Synthesis of ferrierite in presence of Sodium bis-(2-ethylhexyl sulphosuccinate (AOT):

The surfactant used in this method was an anionic surfactant sodium bis-(2-ethylhexyl) sulfosuccinate; AOT (444.45). In a typical synthesis procedure, to 52.5 g

sodium silicate in 25 ml distilled water, 2 ml of pyrrolidine template followed by 1 g of AOT in 10 ml distilled water was added. The mixture was stirred till AOT completely dissolved. Finally 2.4 g of aluminum sulphate hexadecahydrate dissolved in 25-ml water was added followed by remaining 30 ml distilled water. The gel was stirred till homogeneous and then it was transferred to a stainless steel Parr autoclave (300 ml) and heated to 453 K for 50 h. The autoclave was quenched with cold water and the white crystalline solid obtained was filtered, washed, and dried at 373 K for 6 - 8 h. The samples with input SiO_2/Al_2O_3 ratios in the range 25 - 80 were synthesized using the above procedure. The as-synthesized product was then converted to its Na- form by calcining it upto 823 K. The product yield was 9g. The initial gel composition was:

$$20Na_2O : 6.6\,Py : 66\,SiO_2 : Al_2O_3 : 0.47\,AOT : 1600\,H_2O,$$

where Py = pyrrolidine.

2.2.1.5. Non templated synthesis of ferrierite:

The reagents used for the synthesis and their specifications are listed in Table 2.2. This synthesis involved two steps: In the first step, amorphous silica alumina powder was prepared.200 g of silica sol in 40 g was mixed with 15 g of sodium aluminate in 100 ml distilled water under stirring. The gel so formed was transferred to a stainless steel parr autoclave and heated at 363 K for two hrs. The autoclave was then quenched and the material filtered, washed and dried at 373 K. The product was amorphous with particle size of 2μm and SiO_2/Al_2O_3 ratio = 15. The second step involved preparation of two solutions: (i) 17 g of Na_3PO_4 was dissolved in 88 ml distilled water and (ii) 5.05 g of KF was dissolved in 12 ml distilled water. To 53 g of silica alumina powder (prepared in previous step) in 147 ml H_2O, solutions (i) and (ii) were added, the resulting mixture was stirred for 1h. The gel with pH 11.96 was then transferred to a parr autoclave, which was heated at 483 K for 68h. The autoclave was quenched with water; the product was washed, filtered dried at 373 and analyzed by XRD.

2.2.2. Synthesis of Fe- analog of ferrierite:

The reagents used for the synthesis of iron analog of ferrierite are listed in Table 2.4. The synthesis of Fe-FER was conducted following two systems. The first Fe-FER-I

system, involved addition of $Al_2(SO_4)_3.16\ H_2O$ in different concentrations in addition to ferric sulphate, whereas for Fe-FER-II system 0.5 wt. % seed precursors of H/Al-FER have been used.

2.2.2.1. Al+Fe-FER (Fe-FER-I series):

Typical synthesis included, addition of a solution, prepared by mixing 1.32 g of aluminum sulphate hexadecahydrate in 15 g of distilled water, 1.02 g of ferric sulphate dissolved in 10 g of distilled water and 1.8 g of conc. H_2SO_4 in 10 g of distilled water to 52.5 g of Na_2SiO_3 in 25 g of distilled water. This was followed by addition of 10 ml pyrrolidine and remaining 30 ml of distilled water. The bluish gel formed was stirred for approximately 1 h. The gel was transferred to an 300 ml stainless steel autoclave (Parr 4861, 300ml) and heated at 433 K for 40 h. The autoclave was quenched with cold water, the material filtered, washed and dried at 373 K. Utmost care was taken to clean the autoclave to avoid any seeding effect from the previous batches. The samples with SiO_2/Fe_2O_3 ratios ranging from 80 to 240 were synthesized and designated as Fe-FER-I series. The product yield was 7g. The initial gel composition was in the range:

(15.8-95) Na_2O: (31.6-285) py : (0.316-3.0)Al_2O_3 : Fe_2O_3 : (80-240) SiO_2: (633-9494) H_2O

where py = pyrrolidine.

2.2.2.2. Fe-FER (Fe-FER-II series):

In this procedure seeds of a highly crystalline Al-FER were used instead of Al-source. In a typical synthesis 2.06 g of Ferric sulphate dissolved in 10 g of distilled water along with 1.8 g of conc. H_2SO_4 in 10 g of distilled water was added to 52.5 g of Na_2SiO_3 in 25 g of distilled water. The bluish gel formed was stirred for approximately 1 h. To this gel 10 ml of pyrrolidine was added followed by addition of remaining 45 g of distilled water. The gel was stirred for 1 h and finally 0.5 g of highly crystalline H/Al-FER (SiO_2 / Al_2O_3 = 34) were added as seeds. The remaining procedure was same as in the first

method. Fe-FER samples of input gel ratios ranging from 30 to 200 were synthesized by the above procedure and the samples were designated as Fe-FER-II (a - d) series. The product yield was 9g. The gel composition for the second method was in the range:

$$(5.9\text{-}79)\ Na_2O:\ (11.9\text{-}238)py:\ Fe_2O_3:\ (30\text{-}200)\ SiO_2:\ (237\text{-}7920)\ H_2O.$$

where py = pyrrolidine.

2.2.3. Synthesis of Titanium analog of ferrierite (TS-FER):

The synthesis method for pure silica derivative of FER described by Kuperman *et al.*[30], using HF/Pyridine as mineralizing agent has been successfully applied for TS-FER synthesis.

Table 2.4 lists the reagents specifications used in the synthesis of titanium ferrierite. A typical synthesis of TS-FER was as follows: Initially 75.5 g (0.955 mol) pyridine plus 31.5 g (0.533 mol) propylamine plus 3.6 g (0.018 mol) HF/pyridine were mixed in a polypropylene jar under stirring. The resulting clear solution was equally divided into two parts (~ 62 ml each), to one portion 0.5 g (1.47×10^{-3} mol) of tetrabutylorthotitanate dispersed in 5 ml of isopropanol was added and to another portion 6.0 g (0.1 mol) Cab-o-Sil were added and allowed to dissolve. Both the parts were then mixed forming a silico-titanate clear solution under stirring. Finally, 0.5 g of silica-FER seed precursors synthesized according to procedure described Kuperman[30] were added to the entire mixture under continuous stirring to yield uniform dispersion. The resulting solution had a pH 11.0 ± 0.2. This liquid was transferred to a PTFE lined autoclave for crystallizing at 443 K for 60 h under static condition. The crystalline TS-FER was filtered, washed with acetone and dried at 373 K. The dried product was then calcined at 823 K for 48 h. for complete decomposition of the organics and was further characterized. The product yield was 9g. The gel composition was:

$$10.78\ Py:\ 5.45\ PA:\ 80SiO_2:\ TiO_2:\ 1.4\ HF/Py:\ 2.76\ H_2O.$$

where Py = pyridine, PA = propyl amine.

Table 2.4: Reagents used for the synthesis of Fe-FER and TS-FER analog of ferrierite.

Reagents	suppliers	analysis
Ferric sulphate	Loba Chemie	99%
Aluminum sulphate hexadecahydrate $[Al_2(SO_4)_3.16\ H_2O]$	Loba Chemie	99%
Sulphuric acid	S.D. fine Chem. ltd.	98%
Pyrrolidine	SRL	99%
Sodium silicate	-	28% SiO_2; 9% Na_2O
Pyridine	SQ, Qualigens	99%
Propyl amine	E. Merck	99%
HF/Pyridine	Aldrich	75%
Tetra butyl ortho titanate	Aldrich	99%
Isopropanol	S.D. fine Chem. Ltd	99%
Fumed Silica	Cab-O-Sil (Fluka AG)	99%

2.3 Characterization:

The ferrierite materials synthesized above were characterized by the following techniques:

2.3.1 X-ray diffraction (XRD):

The synthesized samples were analyzed by X-ray powder diffraction for quantitative and qualitative phase identification by Rigaku (D Max III VC) using a Ni-filter CuKα radiation (λ = 1.5406 Å) with graphite monochromator and Si as an internal standard. The most crystalline sample in aluminum ferrierite, iron ferrierite and titanium ferrierite was assumed to be 100% crystalline and used as reference. The degree of crystallization of the solid product was estimated from the XRD peak intensity (2θ = 4 - 48°) using the following formula:

$$\% \text{ Crystallinity} = \frac{\text{peak area of the intense peaks of the product}}{\text{peak area of the intense peaks of the standard}} \times 100$$

2.3.2 Scanning electron microscopy:

The morphology and the habit of the synthesized samples was studied using a 440 Stereoscan (Cambridge UK) scanning electron microscope by coating the sample with evaporated Au-Pd film on aluminum sample holder.

2.3.3. Infrared (IR) spectroscopy:

The Fourier transform infrared spectra in the region 400-1400 cm^{-1} were recorded on Nicolet FTIR. Sample was prepared by mixing 0.1 mg of sample 100 mg of potassium bromide (spectroscopic grade) and was palletized in vacuum.

2.3.4. Thermal analysis:

Simultaneous thermoanalytical curves (DTA and TG) were obtained in air with SETRAM TG-DTA 92 analyzer. The sample weight was 40 mg and heating rate was 10 K min^{-1} in air.

2.3.5. Sorption measurements:

Sorption measurements were carried out using conventional gravimetric system consisting of a McBain balance (sensitivity ~ 70 cms, gm^{-1}). 50-70 mg sample was pressed to a pellet and weighed into an aluminum bucket, which was then suspended to a silica spring. The assembly was then evacuated by means of a two stage rotary pump and oil diffusion pump to vacuum of 10^{-6} Torr. The sample was heated slowly to 673 K under vacuum till a constant weight was obtained. The temperature of the sample was lowered to 298 K and the sorbate vapor was admitted to the sample at constant temperature and pressure. The amount sorbed was measured from the extension of the spring, which was recorded after 2 h at each equilibrium pressure using a cathetometer.

2.3.6 Diffuse Reflectance UV-vis spectroscopy:

DRUV-vis spectra were recorded in the range 200 to 800 nm using a Shimadzu UV2101 PC, spectrophotometer with $BaSO_4$ as a reference material. The spectra were recorded in air at 300 K.

2.3.7. Chemical analysis:

The chemical compositions of fully crystalline aluminum, iron and titanium ferrierite in anhydrous form were determined by X-ray Flourescence (3070, Rigaku) using lithium tetraborate as a flux.

2.4. Results and Discussion:

2.4. 1. Synthesis of Al-FER:

2.4. 1.1. Synthesis of Al-FER with pyrrolidine:

Plank *et al.*[3] first demonstrated the synthesis of ferrierite (ZSM-35) with pyrrolidine as template. More recently Kim *et al.*[31] reported synthesis of Ferrierite with pyrrolidine in alkali free media. However, both these synthesis methods required longer crystallization periods. In addition, the application of high temperature, seeding and many other parameters during FER crystallization periods have met with limited success[11,12]. It is also known that addition of mineral acid to a synthesis mixture reduces the crystallization[20]. It has however, recently been shown and generalized[35] that a number of zeolites can be produced within significantly shorter periods using small amount of oxyanions like ClO_4^-, PO_4^{3-} and SO_4^{2-}. From figure 2.1 (a-d), it is evident that the samples obtained are highly crystalline and without any impurity phase. It can also be seen from the figure 2.1 that H-FER synthesized in perchloric acid and phosphoric acid media are highly crystalline (a and b, respectively) as compared to H-FER synthesized in sulphuric acid media (Figure 2.1c) and without acid (Figure 2.1d). The crystallization rate was found to be highest in presence of perchloric acid.

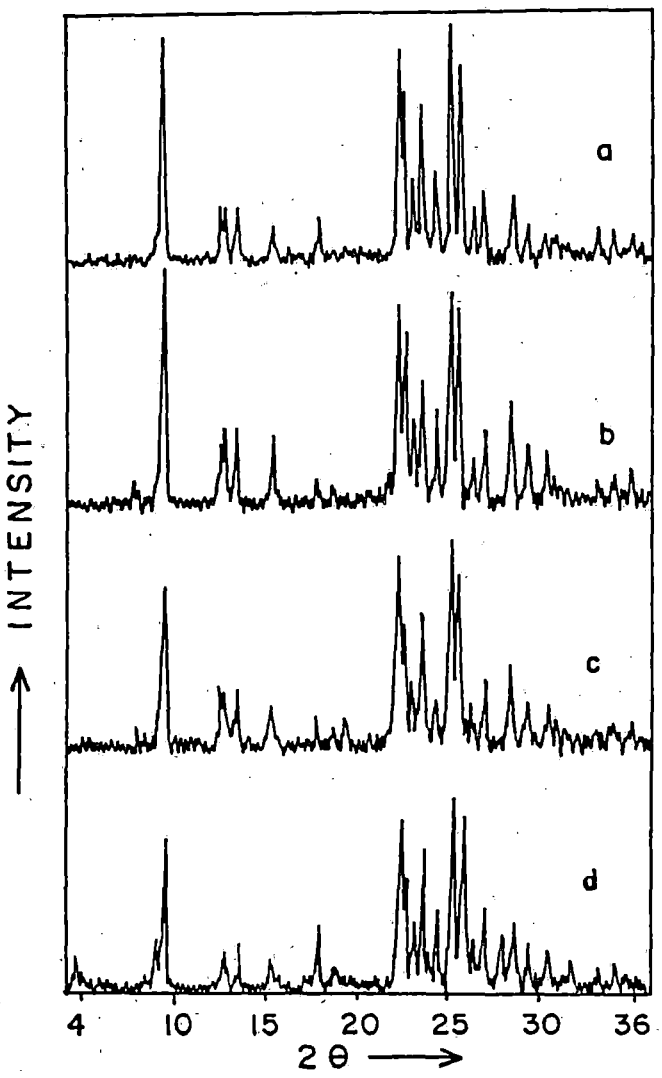

Figure 2.1 XRD patterns of FER (a) Py+$HClO_4$, (b)Py +H_3PO_4 (c)Py+H_2SO_4 (d) no promoter (Py = Pyrrolidine)

2.4.1.1.1. Kinetics of Ferrierite Crystallization:

In order to investigate the nucleation and crystallization kinetics a gel composition

$$20\ Na_2O : 37\ \text{Pyrrolidine} : 66.5\ SiO_2 : Al_2O_3 : 6.3\ P : 1460\ H_2O$$

(where P may be sulphuric, orthophosphoric or perchloric acid) was heated in an autoclave under carefully controlled conditions. The samples were taken out at different intervals of time and the solid product was separated after filtration, washed and dried at 383 K.

The primary reactant mixtures that were used to examine the influence of promoting media (oxyanions ClO_4^-, PO_4^{3-} and SO_4^{2-}) on ferrierite formation are summarized in Table 2.5

Table 2.5: Primary reactant mixtures used for study.

Mixture	moles of promoter/moles of Al_2O_3			gel pH ± 0.2		Temp	Cryst time (h)
	$HClO_4$	H_3PO_4	H_2SO_4	Initial	Final	(K)	
1	10	-	-	11.5	12.6	433	20
2	-	10	-	11.7	12.8	433	30
3	-	-	10	11.6	13.0	433	60
4	none	none	none	12.5	12.5	433	96

The data obtained in the presence of promoter clearly indicates enhanced crystal growth rates for FER system. Figure 2.1 shows typical x-ray powder diffraction patterns of the FER products (synthesis temp. = 433 K) in the presence of promoters. The x-ray patterns show the products to be fully crystalline and pure FER phases, which are in good agreement with the synthetic FER topology[36,37].

The process of zeolite nucleation are usually represented by sigmoid curves (Figure 2.2) which are described by Avrami-Erofeev equation[38-43]:

$$\mathbf{\ln(1/1-\alpha) = (kt)^m} \quad \ldots (1)$$

where α and t are fractional conversion and reaction time, respectively, **k** and **m** are constants. The data from figure 2.2 was fitted to equation (1) and linear plots [lnt Vs $\{\ln(1/1-\alpha)\}$] were obtained. The values of k and m derived from these linear plots are summarized in Table 2.6.

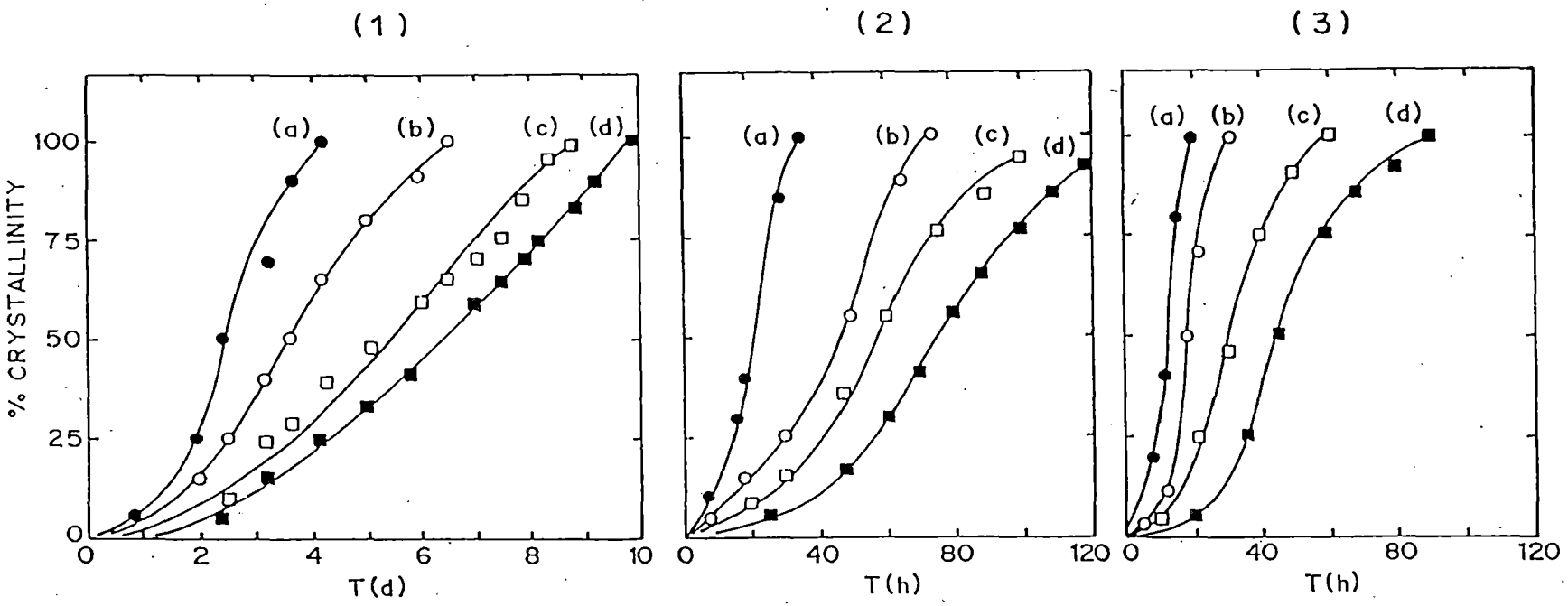

Figure 2.2 The kinetics of crystallization for Ferrierite system at different synthesis temperatures.

Blocks 1-2; 393, 412 & 433 K

Curves (a) to (d); Py+$HClO_4$, Py +H_3PO_4, Py+H_2SO_4 and no promotor

Table 2.6: Avarami-Erofeev parameters for FER synthesis in promoting media.

Synthesis	$HClO_4$		H_3PO_4		H_2SO_4		no promoters	
Temp. K	k x 10^2	m	k x 10^2	m	k x 10^2	m	k x 10^2	m
393	1.4	4.3	0.7	2.4	0.4	1.9	1.7	0.8
413	4.0	3.7	1.7	2.0	1.0	1.3	1.6	0.9
433	5.5	2.9	2.9	1.8	1.1	1.5	1.7	0.8

The values are in accordance with the thermodynamic expectation of a decrease in '**k**' and increase in '**m**' as the temperature of FER synthesis. The increase in '**k**' indicates a faster rate of nucleation and decrease in '**m**' signifies faster crystallization. Table 2.6 also shows that the values of '**k**' and '**m**' obtained when no promoter is used are almost close to a constant value irrespective of synthesis temperature. The slower rate of both nucleation and crystallization in the case of no promoter is probably due to the relatively low condensation ability of the available silicon species in pyrrolidine system under hydrothermal treatment. We believe that in absence of promoter such mechanism (rapid condensation) does not operate and obviously results in an unexpectedly longer crystallization periods[31].

Assuming that the formation of nuclei during the induction period is an energetically activated period, and since the nucleation is the rate determining step, value of apparent activation energies for nucleation (En) and crystal growth (Ec) processes were calculated from the temperature dependence of the rate of nucleation that assumed to be inversely proportional to the induction period;

$$\frac{d[\ln 1/\theta]}{d[1/t]} = \frac{-En}{RT}$$

and Ec was estimated from the inflection point of crystallization step (50 %) linear portion where crystallization rate is the highest;

$$\frac{d[\ln 1/K]}{d[1/t]} = \frac{-Ec}{RT}$$

The values of En and Ec are obtained from linear plots (Figure 2.3) and are summarized in Table 2.7.

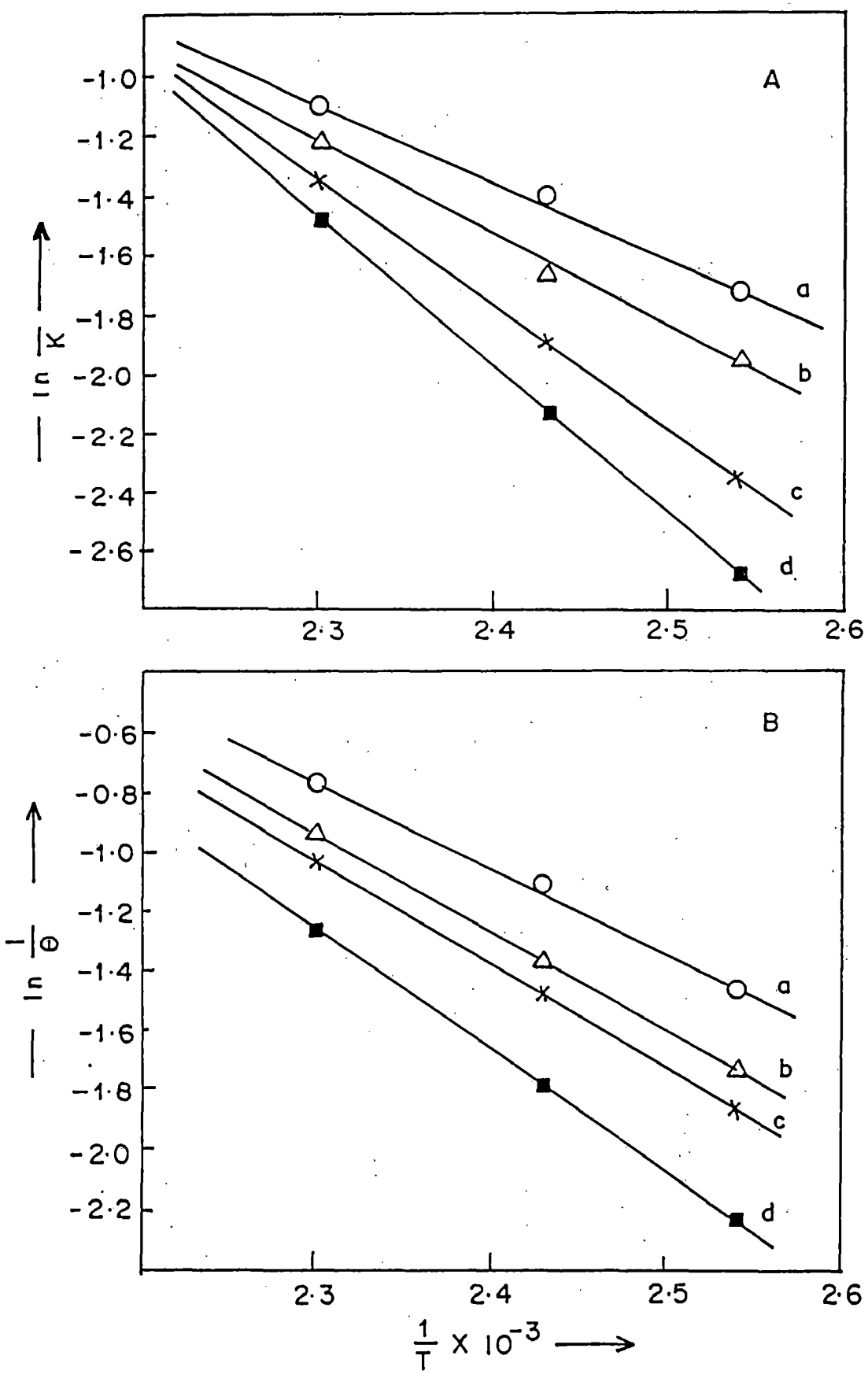

Figure 2.3 Arrhenius plots for (A) nucleation and (B) Crystalization of FER system using promoter media

Table 2.7 : Apparent activation energies for nucleation 'En' and crystallization 'Ec' for FER synthesis.

Sample No.	Promoter medium	gel SiO_2/Al_2O_3	En KJ $mole^{-1}$	Ec KJ $mole^{-1}$
1.	$HClO_4$	66	42	52
2.	H_3PO_4	66	59	60
3.	H_2SO_4	66	200	163
4.	none	66	217	230

The values of En = 42 and 59 KJ $mole^{-1}$, Ec = 52 and 60 KJ $mole^{-1}$ for $HClO_4$ and H_3PO_4 respectively are significantly lower than that for H_2SO_4 and also in the case of no promoter. This clearly demonstrates the enhanced rates of nucleation and crystal growth in presence of promoters (6.3 moles, per mole of Al_2O_3) during FER crystallization. Since these are apparent and not the true values of En and Ec and as they are function of many synthesis parameters including time, pH, temperature, source materials, seed precursors and or promoters (ClO_4^-, PO_4^{3-}, SO_4^{2-}, etc.) no meaningful conclusions could be drawn regarding actual nucleation and crystallization except their relative rates.

It can be seen from the data (Table 2.5) that the crystallization of ferrierite is accompanied by change in the initial pH by nearly 1.0 unit on using $HClO_4$, H_3PO_4 and / or H_2SO_4. The increase in the final pH coincides with the complete crystallization and can be explained in simple terms as a consequence of the incorporation of SiO_2 units into FER framework, which gives rise to an increase in free $[OH^-]/SiO_2$ ratio of the system and thus cause increase in pH. The increased rate of FER crystal growth with rise in pH can be attributed, atleast, in part to much greater concentrations of dissolved species. This helps nuclei to develop more quickly from numerous encounters between precursor species in solution. Kühl[44,45] also reported previously that utilization of silica in an inorganic system increased considerably in the presence of PO_4^{3-} oxyanion. In consideration of this we believe that a similar mechanism may be operating in the FER system when oxyanions of ClO_4^-, PO_4^{3-} and or SO_4^{2-} are generated during crystallization.

Although the exact mechanism and detailed chemistry is not clear, apparently the oxyanions might have a buffering action which controls the pH and depolymerization rate of polymeric silica[46]. The data obtained (Table 2.5) clearly indicates that large ion like ClO_4 with decentralized charge will have weak co-ordination and tend to give higher crystallization rate than that of strongly co-ordinate ions like PO_4^{3-} and / or SO_4^{2-} which might interfere more giving slightly slower crystallization.

2.4.1.1.2. Effect of SiO_2/Al_2O_3 molar ratio in presence of $HClO_4$:

Ferrierite (FER) was synthesized as a crystalline phase at 433 K with SiO_2/Al_2O_3 gel input ratios 30, 66, 90, 150 and 250 using pyrrolidine and having fixed moles (0.0245) of $HClO_4$ in batch composition. Figure 2.4 shows typical kinetic curves while the properties of FER samples obtained are listed in Table 2.8.

Table 2.8 Composition of hydrogel , product and physicochemical properties of Na-FER using promoter (synthesis temperature 433 K)

Sample No	Input gel ratio	Product anhydrous wt. %				crystallinity (%)
		SiO_2	Al_2O_3	Na_2O	SiO_2/Al_2O_3	
1.	30	90.0	5.60	3.5	27.2	100
2.	66	93.0	3.06	3.3	34.6	100
3.	90	96.0	2.53	1.7	40.0	98
4.	150	98.0	1.60	0.5	42	90
5.	250	98.0	1.60	0.5	45	70

The kinetic study reveals relatively higher rate of crystallization (curves 2-4) with lower aluminum proportion in the gel phase. The crystallization rates are found to decrease drastically with increasing aluminum content (curve 5) as well as when there is no promoter (curve 4') in the gel phase. This is believed to be due to the blocking of tetrasiloxysiliane species and subsequently lowering of the condensation phenomena during treatment. However, it was not possible to obtain pure FER with high crystallinity (curve 1 and 2) and moderate yields from the gel phase having SiO_2/Al_2O_3 ratio of 250 and above. This clearly shows that the crystallization rate in presence of promoting medium is dependent on the optimum content of aluminum in the gel phase (upto

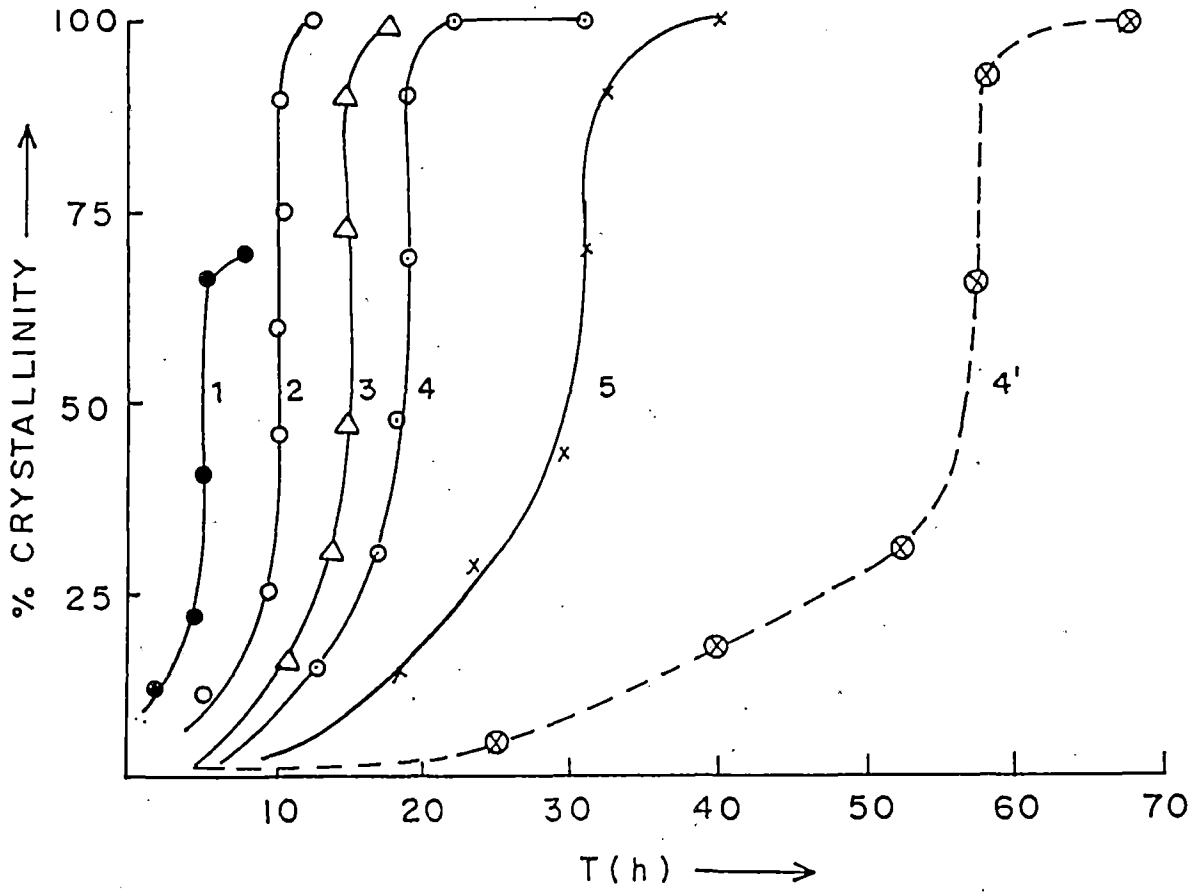

Figure 2.4 The kinetics of crystallization of FER system in Py+$HClO_4$ at 433K, Curves 1-5;

input gel SiO_2 / Al_2O_3 = 250, 150. 99, 66, 30 and none respectively

0.0008 moles of Al_2O_3). Furthermore, the curves 1 and 2 reveals that optimum aluminum content (0.0008) leads to shorter induction period in presence of ClO_4^- anions in the gel phase and accelerates FER crystal growth immediately after induction. In general the FER crystallization rate in presence of $HClO_4$ is inversely related to the aluminum content of the gel and FER can be prepared using a wide range of SiO_2/Al_2O_3 ratios. It is also remarkable, that there is no direct relationship between the value of SiO_2/Al_2O_3 of the gel and the final crystalline product (Table 2.8). The concentration of aluminum atoms in the ferrierite type zeolite is higher than the starting gel. This fact explains the low crystallinity for higher SiO_2/Al_2O_3 ratio (samples 4 and 5, Table 2.8). The FER crystallization in presence of $HClO_4$ initially accelerates and stops when most of aluminum in the gel has been incorporated for framework formation.

2.4.1.2. Synthesis of Al-FER with tetra methyl ammonium hydroxide as template and without Template:

Figure 2.5 displays the XRD patterns of samples synthesized using tetramethyl ammonium hydroxide (TMA-OH) as template. The samples were highly phase pure crystalline materials. Previous reports[9] indicate mordenite as an impurity at low temperature and analcite as an impurity phase at high temperature along with ferrierite. Kibby et al[13] also report synthesis of ferrierite in the presence of TMA-OH at high temperature (573 K) and high pressure. This method, however, produced product with minor impurities. Finally Sorby et al[36] could synthesize pure ferrierite with TMA-OH as templating species at 250° C after 8h. The synthesis method described in section 2.2.1.2; produces pure ferrierite phase at 523 K with good yields of SiO_2/Al_2O_3 ratio in the range of 15 - 25. Table 2.9 describes the physico chemical properties of Ferrierite synthesized by this route (samples 1 and 2). Ferrierite was crystallized in absence of templating agents using phosphates and fluorides samples 3 and 4, Table 2.9. However, the reproducibility with this procedure was difficult. It is evident from the table 2.9, that the

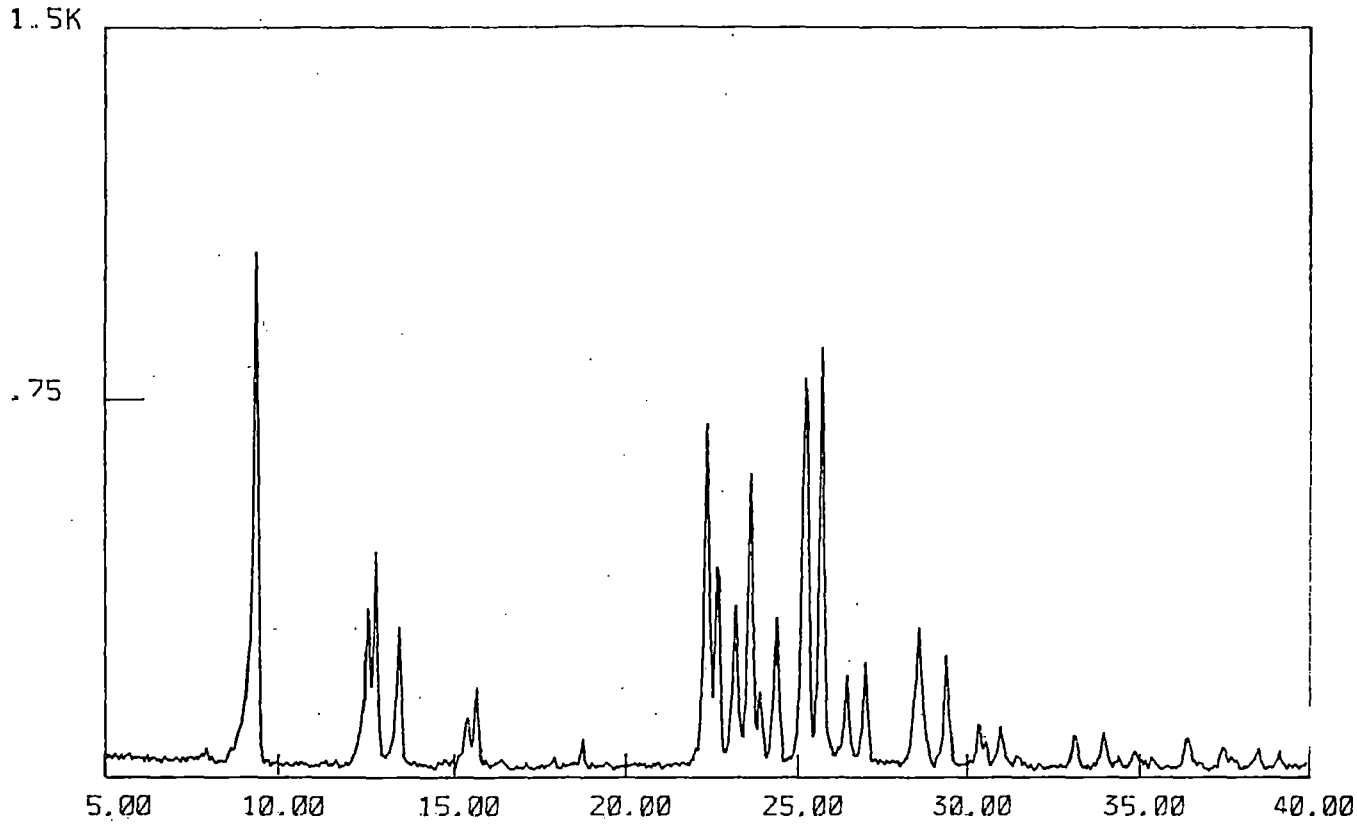

Figure 2.5 X-ray diffraction patterns for samples synthesized using TMA-OH as template

properties of the samples produced by both the procedures are nearly similar. Typically the water sorption is very high indicating hydrophilicity of the sample due to lower silica to alumina ratio. The silica to alumina ratio could not be increased beyond a value of SiO_2/Al_2O_3 of 21 using these routes.

Table 2.9: Physico-chemical properties of Ferrierite synthesized in TMA-OH and without template.

Sample No.	SiO_2/Al_2O_3		Amount adsorbed g/100g of Fe-FER zeolite			Surface Area m^2/g
	gel	zeolite	n-hexane	water	cyclohexane	
1.	20	18	6.64	13.4	0.71	292
2.	15	14	6.78	13.86	0.76	295
3.	19	18	6.88	13.85	0.67	300
4.	23	21	6.85	13.84	0.83	298

2.4.1.3. Synthesis of ferrierite in Sodium bis-(-2 ethylhexyl) sulphosuccinate (AOT)/pyrrolidine system:

Table 2.10 summarizes the physico-chemical properties of ferrierite synthesized using pyrrolidine/AOT system. Ferrierite samples with SiO_2/Al_2O_3 ratios in the range 30 to 80 were synthesized. Figure 2.6 (a-c) represents the XRD patterns for ferrierite samples synthesized in presence of AOT (sample nos. 2, 4 and 6, Table 2.10). The samples were found to be highly crystalline without any impurity phase. Ferrierite samples with high output SiO_2/Al_2O_3 ratios could be synthesized (Table 2.10, sample 4) by this method. However, when SiO_2/Al_2O_3 ratio was increased above 250, ferrierite crystallized with poor yields. Catalytic amount (0.02 moles) of pyrrolidine was found to be necessary for ferrierite synthesis when AOT (0.0009-0.0025 moles) was used in the synthesis gel, otherwise mixed phase i.e. FER + ZSM-5 were formed (Table 2.10, sample 5). Ferrierite crystallized in 0.02 moles of pyrrolidine alone but the yield was found to be very low (Table 2.10, sample 8). However, addition of AOT under similar conditions was found to improve the yield as well as FER with higher SiO_2/Al_2O_3 could be crystallized.

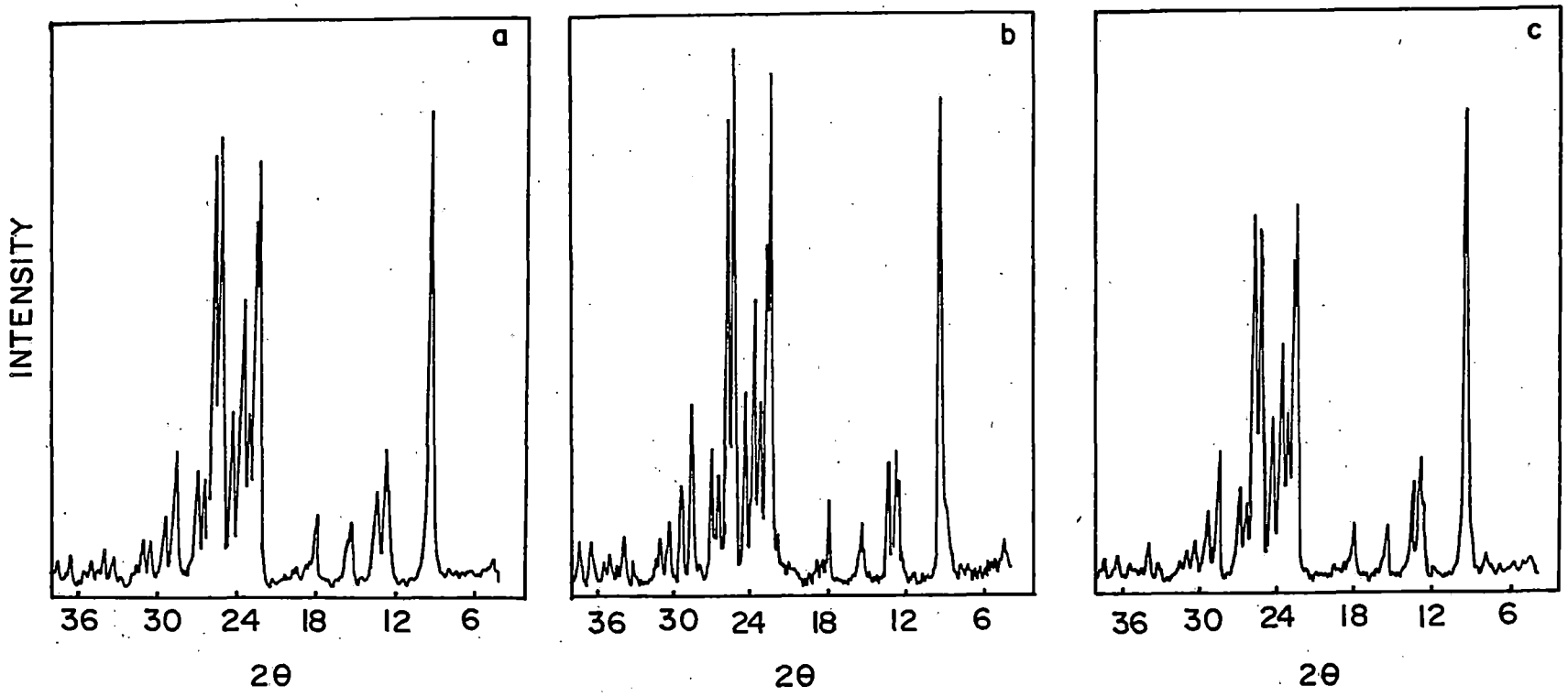

Figure 2.6 X-ray diffraction patterns for samples synthesized in presence of AOT

(a) SiO_2 / Al_2O_3 = 40 (b) SiO_2 / Al_2O_3 = 80 and (c) with low AOT

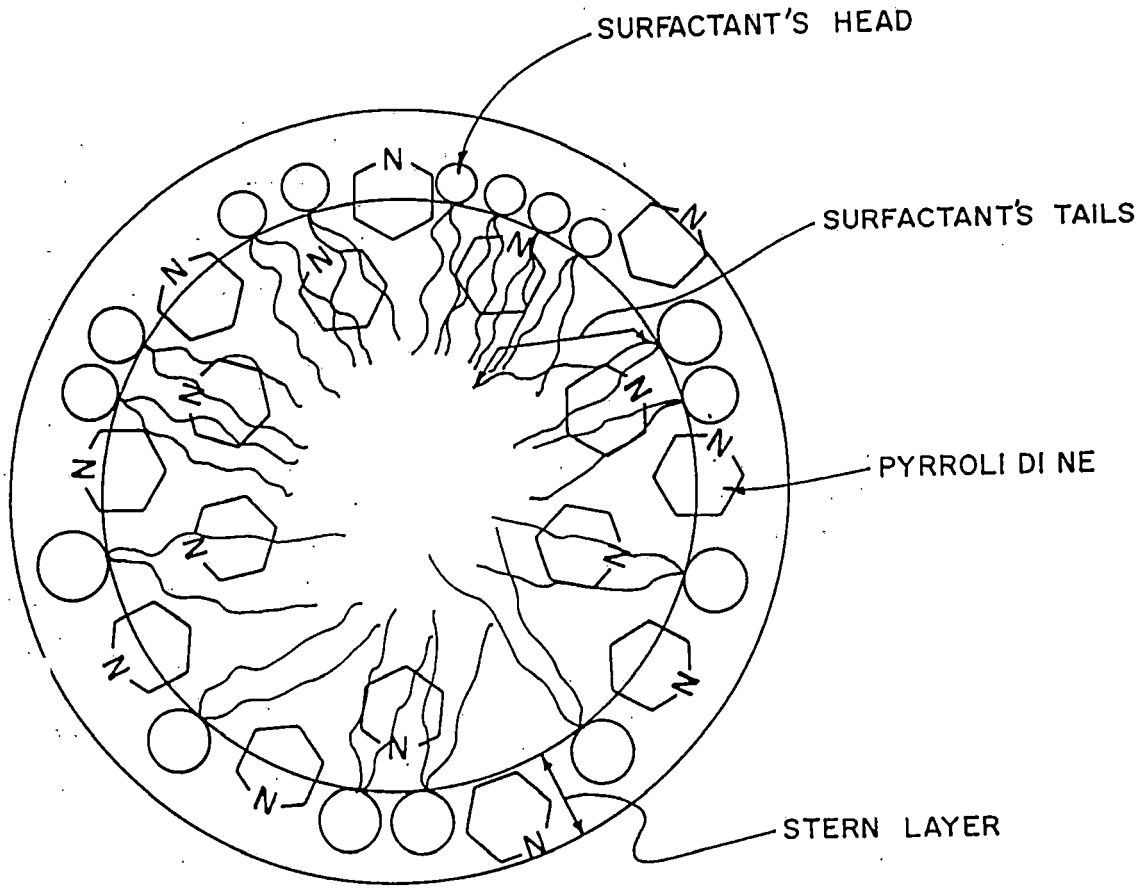

Figure 2.7 Schematic representation of microdroplet formation in the gel system containing water/AOT/pyrrolidine and salts. The pyrrolidine molecules are concentrated in and around the stern layer.

Table 2.10: Physico-chemical properties of samples synthesized in AOT/pyrrolidine system.

Sample No.	SiO_2/Al_2O_3 gel	SiO_2/Al_2O_3 product	AOT (moles)	Pyrrolidine (moles)	Product	yield %
1.	66	32	-	0.1197	FER	60
2.	40	30	0.0025	0.0253	FER	60
3.	66	48	0.0025	0.0253	FER	65
4.	80	68	0.0025	0.0253	FER	62
5.	60	-	0.0025	-	FER + ZSM-5	-
6.	60	50	0.0009	0.0253	FER	52
7.	60	52	0.0017	0.0253	FER	58
8.	60	30	-	0.0253	FER	15

2.4.1.3.1. Role of AOT:

The concentration of surfactant (AOT) was above CMC (critical micelle concentration) value. The formation of milky emulsion indicated formation of microdroplets, which are beyond the range (larger size) of microemulsion. The core of a microdroplet is the non-polar region and stern layer is the polar region. The polar-polar and non-polar-non-polar interactions orient pyrrolidine molecule in a particular fashion as shown in figure 2.7. This type of arrangement may increase the interaction between pyrrolidine and silicate and or aluminum species and induce orientation in pyrrolidine molecules to interact with Si and or Al species. The excess quantity of pyrrolidine molecules required as "*space filler*" was thus avoided due to micro-droplet formation. This may be the reason for requiring catalytic amounts of pyrrolidine during the FER crystallization.

2.4.2. Synthesis of ferrisilicate analog of ferrierite (Fe-FER):

Samples of Fe-FER system were prepared by two methods[46a]. The samples prepared by the first method *i.e* Fe-FER-I (a-d) series were synthesized by partly substituting Fe^{3+} for Al^{3+}. Pure crystalline Fe-FER could be obtained for SiO_2/M_2O_3 (M= Fe + Al) ratio of 60 and SiO_2/Fe_2O_3 ratio between 80-240. It was observed that as the concentration of Fe^{3+} in the starting gel was increased and that of Al^{3+} was decreased, the

metastability for ferrierite phase decreases and ZSM-5 appears as an impurity phase (Table 2.11).

While in the case of the second method in absence of added aluminum, small quantity (0.5 g) of highly crystalline H-Al-FER (SiO_2/Al_2O_3 = 32) were added as seeds and pure Fe-FER could be crystallized in the SiO_2/Fe_2O_3 range of 30 to 100 (input). These samples were designated as Fe-FER-II (a-d). Figure 2.8 (A, B) shows the X-ray diffraction patterns for both as synthesized and calcined (i) Al-FER, (ii) Fe-FER-I and (iii) Fe-FER-II which are found to be in good agreement with those reported for FER phase. It was observed that total replacement of Al^{3+} by Fe^{3+} could not be achieved in the absence of seeds and led to the formation of ZSM-5, indicating that some optimum quantity of Al^{3+} ions is necessary to stabilize the ferrierite type topology. On calcination the intensity of low angle peaks in the XRD patterns (in case of all the samples) was found to increase, which may be due to the removal of organic moieties from the voids of the FER and the samples were found to develop a slight buff color. The other changes observed may be due to minor variation in the lattice constants. The lattice parameters were verified using least square fitting.

Table 2.11: Physico-chemical properties of Fe-FER series.

Sample*	gel		zeolite		K/Fe	%
	$SiO_2/^{\dagger}M_2O_3$	SiO_2/Fe_2O_3	SiO_2/M_2O_3	SiO_2/Fe_2O_3	molar ratio	cryst.
Fe-FER-Ia	60	80	32	42	0.65	90
Fe-FER-Ib	60	120	34	63	0.68	95
Fe-FER-Ic	60	240	30	124	0.70	89
Fe-FER-Id	no added Al	60	no added Al	32	N.D	75 + ZSM-5
Fe-FER-II a	no added Al	40	no added Al	25	0.81	85
Fe-FER-II b	—do—	60	—do—	34	0.86	95
Fe-FER-II c	—do—	90	—do—	37	0.80	92
Fe-FER-II d	—do—	100	—do—	40	0.78	90

* note: Fe-FER-I series without seeds and Fe-FER-II series are with seeds.

† $M_2O_3 = Al_2O_3 + Fe_2O_3$

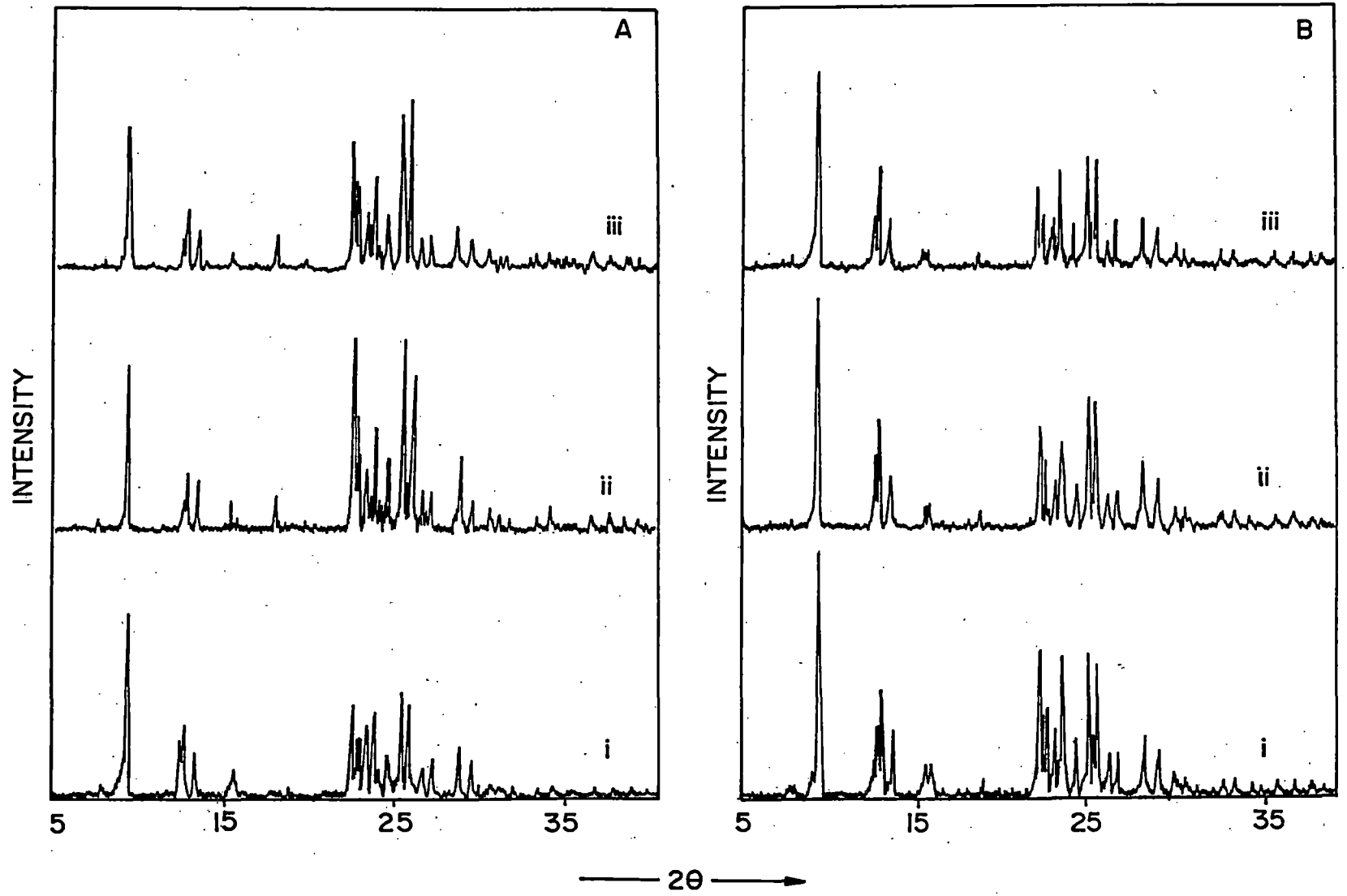

Figure 2.8 X-ray diffraction pattern for (A) as-synthesised & (B) Calcined samples (i) Al-FER (ii) Al+Fe-FER and (iii) Fe-FER

Least square analysis data and the computed values of the unit cell volume from the XRD data (Table 2.12) reveal expansion of unit cell of Fe-FER-I and II series indicating successful insertion of Fe-ions during hydrothermal synthesis. The ion-exchange capacities for Fe-FER-I and Fe-FER-II series are summarized in Table 2.11. It is observed that the ion-exchange capacities of Fe-FER-I series were lower as compared with Fe-FER-II indicating presence of higher number of exchangeable sites for the II series. It is known from the literature[47] that K/Fe molar ratio near unity indicates tetrahedral location capable for ion exchange in ferrisilicates. Considering this, Fe-FER-I indicates nearly 25% loss of ion exchange sites on calcination (Table 2.11). However, closer values to unity for Fe-FER-II attests that the larger portion of substituted Fe can be located in sites capable for ion exchange.

Table 2.12: Data on unit cell parameters for Fe-FER series.

Sample	Unit cell parameters (Å)			Unit cell
	a_o	b_o	c_o	volume (Å) cm^3
Al-FER	18.82	14.06	7.43	1957
Fe-FER-Ib	18.88	14.10	7.44	1980
Fe-FER-IIb	18.97	14.13	7.45	1997

2.4.3. Synthesis of Titanium analog of Ferrierite (TS-FER):

A number of samples of TS-FER system were prepared with different Si and Ti contents[48]. Table 2.13 lists the chemical composition of the initial mixture and the corresponding products. For all the samples Ti : Si ratios were higher in the product than in the initial mixture, indicating that not all the silica was involved in the crystallization process. TS-FER was expected to crystallize more readily along with Ti-butoxide and make Si-O-Ti oligomers, however, the reaction mixture in which both SiO_2 and Ti-butoxide were co-hydrolyzed did not form any FER crystals even after 15 - 30 days heating, but transformed to ZSM-39 phase in contrast to the pure Si- derivative synthesis in which highest crystallinity for FER phase was attained in 5 days under identical

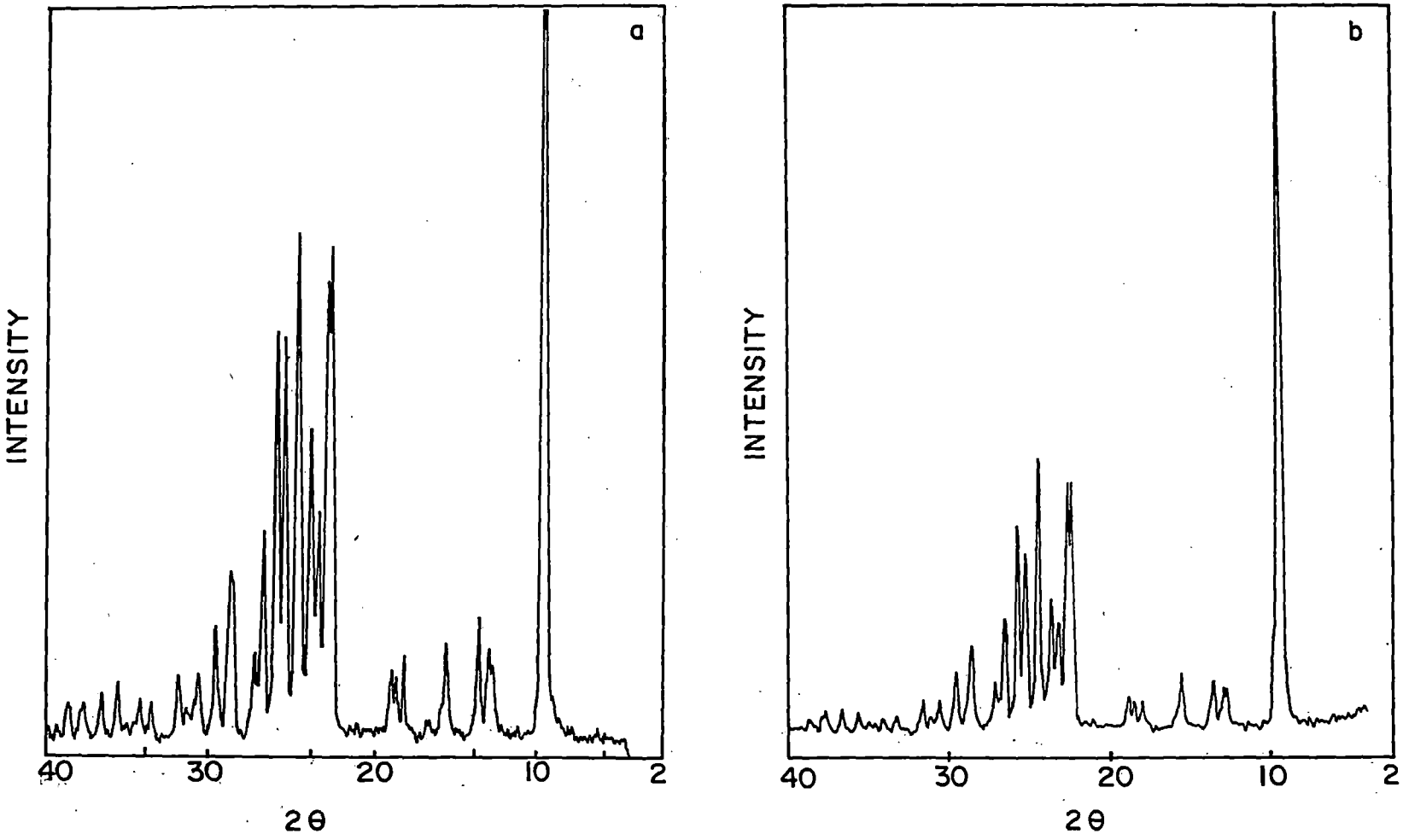

Figure 2.9 X-ray diffraction pattern for silicalite analog of Ferrierite (A) as-synthesised & (B) calcined form.

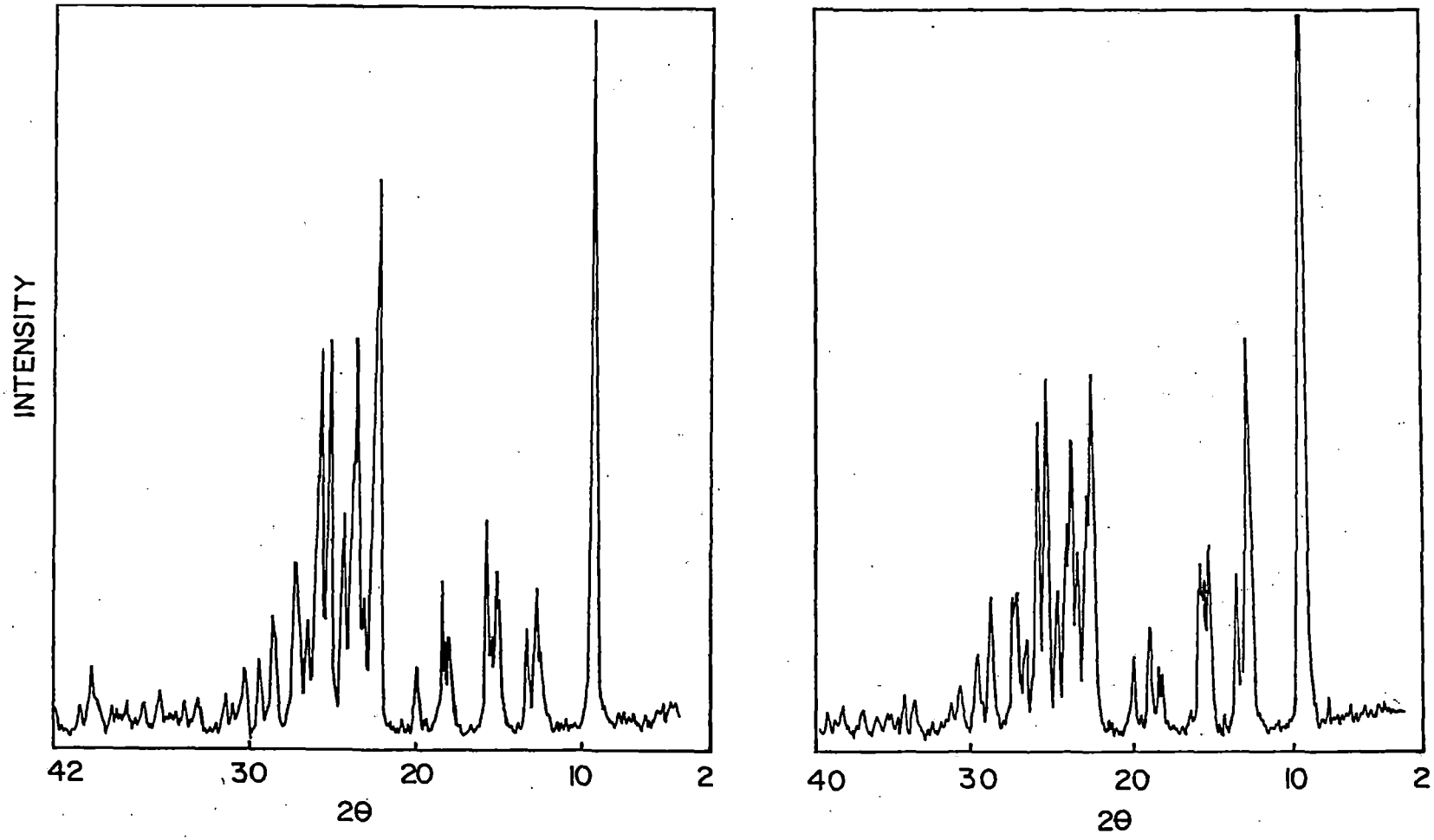

Figure 2.10 X-ray diffraction pattern for TS-FER (A) as-synthesised & (B) calcined forms

conditions. These findings indicate that the presence of Ti^{4+} ions tends to impede and lower the nucleation rates in organothermal TS-FER system. It was, however, found that adding seed crystals of Si-FER derivative in small quantity (0.8 - 1.0 wt.% of gel mix) accelerates both nucleation and crystallization. It can be seen (Table 2.13) that in no case framework titanium in excess of 1.8% was found. These results indicate that there exits a upper limit of framework titanium (Ti^{IV}) incorporation (maximum of 2.0 wt.%) and formation of extra framework (Ti^{IV}) in the form of TiO_2 when Ti concentration is increased up to 50 mole percent of Si input moles (Sample No. 4). Figure 2.9 a and b show the x-ray diffraction pattern of as-synthesized and calcined siliceous ferrierite synthesized under organothermal synthesis conditions. X-ray diffraction patterns of titanium analog of ferrierite in its as-synthesized as well as calcined form are shown in figure 2.10 (a and b). On comparison it can be seen that all the samples are highly crystalline and maintain their structural integrity on calcination.

Incorporation of Ti^{4+} ions into the framework would generally cause a unit cell volume variation. Based on this, the unit cell volumes of series of samples as calculated from XRD data are presented in Table 2.13. The unit cell volume of sample no. 1 showed a marked increase (1977.78 $Å^3$) in comparison with that of pure silica FER derivative (1947.96 $Å^3$).

Table 2.13: Physico-chemical properties of TS-FER

Sample	gel (moles)		product	Unit Cell Parameters			U.C.V	Ti
No.	Si	Ti	Ti/Si	a_o	b_0	c_0	$(Å)^3$	Wt.%
1	0.1	1.2×10^{-3}	1.6×10^{-2}	18.945	14.062	7.424	1977.78	1.8
2	0.1	8.3×10^{-4}	9.0×10^{-3}	18.900	14.061	7.422	1972.41	1.5
3	0.1	5.5×10^{-4}	6.0×10^{-3}	18.829	14.061	7.419	1964.20	1.2
4	0.1	0.05	FER+ major anatase	ND	ND	ND	ND	ND
5	0.1	no Al/Ti	-	18.687	14.062	7.413	1947.96	no Al/Ti

2.5: Conclusion:

- Ferrierite synthesis was optimized using various templates like pyrrolidine and tetramethylammonium hydroxide. It was observed that with pyrrolidine as a template ferrierite crystallized upto a ratio of 48, while with TMA-OH a maximum SiO_2/Al_2O_3 ratio of 20 could be obtained.
- Ferrierite was synthesized for the first time in presence of promoting media (viz. ClO_4^-, PO_4^{3-} and SO_4^{2-}), which thereby reduced the crystallization time. The crystallization rate was maximum in presence of perchloric acid and minimum in the case of sulphuric acid media.
- Ferrierite crystallization kinetics were studied and they revealed that the energy of activation for perchloric acid media was minimum hence faster crystallization.
- Ferrierite was, for the first time, synthesized in presence of an anionic surfactant, sodium bis-(-2 ethyl hexyl) sulphosuccinate, thus reducing the consumption of pyrrolidine by one sixth.
- Ferrisilicate analog of ferrierite was synthesized by seeding method and in presence of pyrrolidine template.
- Titanosilicate analog of ferrierite has been synthesized for the first time under organothermal synthesis conditions.

2.6. References:

1. Meier, W.M. and Olson, D.H.; 'Atlas of Zeolite Structure Types'; *Zeolites* **12** (1992) 5.
2. Vaughan, P.A.; *Acta Cryst.* **21** (1966) 983.
3. Plank, C.J; Rosinski, E.J. and Rubin, M.K.; US Pat. 4, 016, 245 (1977) assigned to Mobil Oil Corp..
4. Plank, C.J; Rosinski, E.J. and Rubin, M.K.; US Pat. 4, 046, 859 (1977) assigned to Mobil Oil Corp.
5. Plank, C.J.; Rubin, M.K. and Rosinski, E.J; US Pat. 4,105,541 (1978) assigned to Mobil Oil Corp.
6. Kokotailo, G.T.; Schlenker, J.L; Dwyer, F.G. and Valyocsik, E.W.; *Zeolites* **5** (1985) 349.
7. Seddon, D. and Whittam, T.V.; EPA 55, 529 (1981) assigned to ICI.
8. Barrer, R.M. and Marshall, D.J.; *J. Chem. Soc.* (1964) 2296.

9 a. Coombs, D.S.; Ellis, A.J.; Fyfe, W.S. and Taylor, A.M.; *Geochem Cosmochim Acta* **17** (1959) 53.

b. Sanderov, E.E.; *Geokimiya* **9** (1959) 820

c. Sands, L.B.; Int. Conf. Mol. Sieves (1967) p 71.

10. Hawkins, D.B.; *Mater. Res. Bull.* **2** (1967) 951.
11. Vaughan, D.E.W. and Edwards, G.C.; USP 3, 966, 883 (1976) assigned to W.R. Grace.
12. Winquist, B.H.C.; USP 3, 933, 974 (1976) assigned to Shell Oil Corp.
13. Kibby, C.L.; Perotta, A.J. and Massoth, J.; *J. Catal.***35** (1974) 256.
14. Kaduk, J.A.; USP 4, 323, 481 (1982) assigned to Standard Oil Comp. (Indiana).
15. Marosi, L.; Schwarzmann, M. and Stabenow, J.; EPA 49, 386 (1981) assigned to BASF.
16. Martin D.E.; G. Offenl, 2, 507, 426 (1975) assigned to BP.
17. Nanne, J.M.; Post, M.F.M. and Stork, W.H.J.; EPA 12, 473 (1979).
18. Taramasso, M.; Perego, G. and Notari, B.; Fr. P. 2, 478, 063 (1981) assigned to Snamprogetti.
19. Araya, A and Lowe, B.M; *J.Chem. Res.* **5** (1985) 192.
20. Valyoscik, E.W. and Rollmann, C.D.; *Zeolites* **5** (1985) 192.
21. Borade, R.B. and A. Clearfield; *Zeolites* **14** (1994) 458.
22. Xu, W.; Dond, J. X.; Li, J.; Ma, J. and Dou, T.; *Zeolites* **12** (1988) 299.
23. Seddon, D. and Whittam, T.V.; Eur. Pat. B-55 529 (1985).
24. Whittam, T.V.; Eur. Pat. A 103 981 (1984).
25. Schreyeck, L.; Caullet, J.C.; Mougenel, J.C.; Guth, J.L. and Marler, B.; *J. Chem. Soc. Chem. Commun.* (1993) 2187.
26. Chang, C.D.; Hellring, S.D. US Pat. 5, 288, 475 ( ) Mobil Oil Corp.
27. Forber, N.R.; Rees, L.V.C.; *Zeolites* **15** (5) 444.
28. Hellring, S.D.; Chang, C.D.; Lutner, J.D.; US Pat. 5, 190, 736 ( ) Mobil Oil Corp.
29. Gies, H. and Gunawardane, R.; *Zeolites* **7** (1987) 442.
30. Kuperman, A; Nadami, S.; Oliver, S.; Ozin,G.A.; Graces, J.M. and Olken, M.M, *Nature* **365** (1993) 239.

31. Kim, T.J.; Ahm, W.S.; Hong, S.B.; *Microporous Materials* 7 (1996) 35.

32. Sulikowsler, B and Klinnowski, J.; *J.Chem. Soc. Chem. Commun.* (1989) 1289.

33. Jacob, N.E.; Joshi, P.N.; Shaikh, A.A. and Shiralkar, V.P.; *Zeolites* **13** (1993) 430.

34. Borade, R.B. and Clearfield, A.; *J. Chem. Soc. Commun.* (1996) 2267.

35. Kumar, R.; Bhaumik, A.; Ahedi, R.K. and Ganapathy, S.; *Nature* **381** (1996) 298.

36. Fjelhag, H.; Lilerud, K.P.; Norby, P. and Sorby, K.; *Zeolites* **9** (1989) 152.

37. Jacobs, P.A. and Martens, J.A.; 'Synthesis of High Silica Aluminosilicate Zeolites' *Stud. Sci. Surf. Catal.* (Elsevier, Amsterdam) **33** (1987) 218.

38 Avrami, A.J.; *J. Chem. Phys.* **9** (1941) 177 ; B.V. Erofeev, C.R.; *Acad. Sci.* U.S.S.R **52** (1945) 511

39. Kotasthane, A.N.; Shiralkar, V.P.; Hegde, S.G. and Kulkarni, S.B.; *Zeolites* **6** (1986) 233.

40. Rao, G.N.; A.N. Kotasthane and Ratnasamy, *Zeolites* **9** (1989) 483.

41. Joshi, P.N.; A.N. Kotasthane and Shiralkar, V.P.; *Zeolites* **10** (1990) 598.

42. Awate, S.V.; Joshi, P.N.; Shiralkar, V.P. and Kotasthane, A.N.; *J. Inclusion Phenomena and Molecular Recognition in Chemistry* **13** (1992) 207.

43. Tian, H. and Li, C.; Proc. presented in 11th Int. Zeo. Conf. Seoul (1996).

44. Kühl, G.H.; *J. Inorg. Nucl. Chem.* **33** (1971) 3261.

45. Kühl, G.H.; *J. Inorg. Chem.* **10** (1971) 2488.

46. Brick, DEW.; *'Molecular Sieves'* (Wily, New York) (1974) 328.

46a. Shevade, S.S.; .Ahedi, R.K and Kotasthane, A.N.; *Catalysis letters* , **49** (1997) 69-75.

47. Szostak, R., Nair, V.and Thomas, T.L.; *J. Chem. Soc., Faraday Trans. 1*, **83** (1987) 487.

48. Ahedi, R.K. and Kotasthane, A.N.; *J.Mat.Chem* **8** (1998) 1685.